Journal of Materials Chemistry C

ROYAL SOCIETY OF CHEMISTRY

COMMUNICATION

View Article Online
View Journal | View Issue

Cite this: J. Mater. Chem. C, 2025, 13, 16929

Received 16th June 2025,
Accepted 29th July 2025

DOI: 10.1039/d5tc02326b

rsc.li/materials-c

Thermochromism *versus* piezochromism in $(PMA)_2CuX_4$ (X = Br, Cl) halide perovskites

Rafał Bartoszewicz, *[a] Jan-Albert Zienkiewicz, [b] Sri Hartati, [c] Arramel Arramel, [c] Jan Kopaczek, [a] Muhammad Danang Birowosuto [b] and Robert Kudrawiec [a]

This study addresses the challenges of poor thermodynamic and structural stability in copper-based perovskites under extreme conditions. By replacing hygroscopic cations with hydrophobic ones like phenylmethylammonium (PMA), the stability of these materials is significantly enhanced. Two-dimensional copper-based perovskites, $(PMA)_2CuCl_4$ and $(PMA)_2CuBr_4$, are examined for their large band gap tunability, focusing on thermo- and piezo-chromism. Temperature-dependent transmission and reflectance measurements show that the band gaps narrow by ~70 nm (from 466 to 536 nm) for $(PMA)_2CuCl_4$ and by ~87 nm (from 472 to 559 nm) for $(PMA)_2CuBr_4$ across the temperature range of 20–320 K. Pressure-dependent transmission reveals that a redshift in the band gap occurs, shifting from 476 to 546 nm (~70 nm) up to 10.94 GPa for $(PMA)_2CuCl_4$ and from 482 to 572 nm (~90 nm) up to 10.86 GPa for $(PMA)_2CuBr_4$ under ambient conditions. These changes are reversible, confirming the stability under extreme conditions. The observed significant thermo- and piezo-chromic effects make the materials very functional for use in color tuning and temperature and pressure sensor applications. Additionally, the comparison of thermo- and piezo-chromism shows that even if electron–phonon interactions play an important role in both phenomena, the changes in lattice parameters induced by temperature (expansion) and pressure (compression) are fundamentally different, leading to distinct mechanisms of energy gap narrowing.

1 Introduction

Two-dimensional (2D) lead halide organic–inorganic perovskites have received considerable attention in recent years due to their large exciton binding energy, high photoluminescence quantum yield, and versatile exciton radiative recombination processes, which are desirable for micro/nano-lasers and high-efficiency light-emitting diodes (LEDs).[1–12] However, the widespread use of lead-based perovskites is hindered by the toxicity of the lead component, limiting their commercial applications in optoelectronic devices. In order to optimize the utility of perovskites, researchers have explored alternatives by replacing the toxic Pb with environment-friendly elements, including Sn(II), Ge(II), Bi(II), Sb(II), and the transition metal Cu(II).[13–18] Among these, Cu, a low-cost, earth-abundant, and non-toxic element, has emerged as a promising substitute for Pb in 2D perovskite materials. Cu-based perovskites have demonstrated similar or superior electronic and optical properties compared to Pb-based perovskites, including efficient charge transportation in metal-halide octahedral layers, high thermodynamic stability, low-cost synthesis, and environmental inertness, making them suitable for commercial applications.[16,19,20] Despite these facts, key challenges remain for Cu-based perovskites, such as limited absorption coefficient and insufficient long-term stability.[16] One promising strategy to overcome these limitations involves replacing hygroscopic cations with more hydrophobic cations, like phenylmethylammonium (PMA), which enhances material stability under extreme conditions, including exposure to heat, pressure, UV light, and humidity,[21,22] but further studies of these compounds are still needed.

Piezochromism involves color or luminescence changes under pressure and has gained interest in crystalline systems such as halide perovskites and metal–organic frameworks. So far, only a limited number of studies have explored crystals of perovskites under high pressure.[23–25] In addition, thermochromism refers to the reversible color change of materials in response to temperature variations. This property has attracted increasing interest for applications in smart coatings,[26] energy-saving systems,[27] and temperature sensors.[28] Thermochromic materials are also useful in environments where conventional temperature monitoring is difficult.[29] In hybrid perovskites, thermochromism is often linked to structural changes, including lattice distortion. For example, copper-based layered perovskites

[a] Department of Semiconductor Materials Engineering, Wroclaw University of Science and Technology, Wybrzeże Wyspiańskiego 27, 50-370 Wrocław, Poland. E-mail: rafal.bartoszewicz@pwr.edu.pl
[b] Lukasiewicz Research Network-PORT Polish Center for Technology Development, Stabłowicka 147, 54-066 Wrocław, Poland
[c] Center of Excellence Applied Physics and Chemistry, Nano Center Indonesia, Jalan Raya PUSPIPTEK, South Tangerang 15314, Indonesia

show reversible transitions from orange to red, while inorganic compounds like $Cs_3Sb_2I_9$ and $Cs_2AgBiBr_6$ shift from red to brown with temperature.[30–32]

Copper-based halide perovskites, such as $(PMA)_2CuCl_4$ and $(PMA)_2CuBr_4$, are promising materials for applications in solar cell absorbers, scintillators, and LEDs.[33,34] To recognize their utilities in mentioned applications as well as other applications, it is essential to examine their behavior under varying temperature and hydrostatic pressure conditions. The flexible crystal structures of perovskites, combined with significant lattice expansion induced by temperature, provide a viable approach to modulate the material properties in a controlled manner, such as tuning the band gap.[35–37] Understanding the effects of temperature and hydrostatic pressure on these materials is crucial, as both factors can induce significant changes in the crystal structure. This opens new possibilities for copper-based hybrid perovskites to be used as thermometers or impact/stress indicators, thanks to their color and electronic conductivity changes upon temperature and pressure variations.[35,38]

While absorption (α) and reflectance (R) have been extensively studied under varying temperature or hydrostatic pressure conditions for various 2D perovskites,[10,39–48] such studies are rare for copper-based hybrid perovskites. Moreover, there are no reports on temperature-dependent experiments for $(PMA)_2CuCl_4$ and $(PMA)_2CuBr_4$ specifically and no studies on the effect of pressure on $(PMA)_2CuCl_4$.

In this article, we investigate the thermo- and piezo-chromic properties of $(PMA)_2CuCl_4$ and $(PMA)_2CuBr_4$ perovskites. Absorption and reflectance spectra show a temperature-induced redshift of the absorption edge, consistent with band gap narrowing in both investigated perovskites. Similarly, pressure-driven transmission measurements reveal a redshift of the absorption edge under increasing hydrostatic pressure, leading to a visible color change. Moreover, the fundamental energy gap for both was found to be indirect.

2 Results and discussion

Prior to discussing the thermo- and piezo-chromic properties of the $(PMA)_2CuCl_4$ and $(PMA)_2CuBr_4$ perovskites, we first characterized the crystallinity order, vibrational properties, and chemical states of the compounds using X-ray diffraction (XRD), Fourier transform infrared spectroscopy (FTIR), Raman spectroscopy and X-ray photoemission spectroscopy (XPS). The structural characterization of the studied perovskites confirmed their high quality. In particular, the structural order of the 2D Ruddlesden–Popper (RP) phase according to its XRD analysis and inorganic network connectivity and optimized geometric calculations. A detailed description of the experimental results, analysis and methods is provided in Fig. S1–S14 in the SI.

2.1. Thermochromism in $(PMA)_2CuBr_4$ and $(PMA)_2CuCl_4$ halide perovskites

After successful synthesis and fundamental structural characterization under ambient conditions, absorption (α) and reflectance (R) spectra were measured for both perovskites as a function of temperature to investigate their thermochromism. Fig. 1(a) shows the absorption spectra of $(PMA)_2CuBr_4$ as a function of temperature, measured between 20 and 320 K, to analyze the temperature dependence of the fundamental energy gap, while Fig. 1(b) presents the R spectra measured in the range of 30 to 320 K.

From the α measurements, it was observed that the energy gap narrows linearly with increasing temperature for both the direct and indirect band gaps, as shown in Fig. 1(c). Specifically, the energy gap decreases by 342 meV ($\sim$63 nm from 450 to 513 nm) for the direct gap and 426 meV ($\sim$87 nm from 472 to 559 nm) for the indirect gap, respectively, between 20 and 320 K. This exceeds the narrowing typically observed for group III–V semiconductors (70–90 meV)[49] and other perovskites measured in the same temperature range.[50,51] Such a significant temperature-dependent narrowing of the energy gap also leads to visible thermochromism, where the material undergoes a noticeable color change with increasing temperature. As the energy gap decreases, the material absorbs light at different wavelengths, resulting in a visible change in color, from green at 20 K to yellow at 320 K. The reduction in the energy gap and the change in the color of the studied samples are also confirmed by R measurements. However, due to the presence of a transparency region near the indirect transition, accurately determining the transition energy at each temperature was challenging.

As in other semiconductors, the narrowing of the energy gap with increasing temperature is related to lattice expansion and enhanced electron–phonon interactions.[52] The temperature dependence of the band gap can be typically described using the Varshni relation[53]:

$$E_0(T) = E_0(0) - \frac{(\alpha T^2)}{(\beta + T)} \quad (1)$$

where $E_0(0)$ is the energy of the optical transition at $T = 0$ K, and α and β are the material constants. This relation is non-linear at low temperatures but becomes nearly linear when $T \gg \beta$, allowing for a linear approximation as the first-order approach.

To determine the nature of the absorption edge (whether related to a direct or an indirect band gap), the α^2 and $\sqrt{\alpha}$ spectra were compared with the R spectra. From this comparison, it was concluded that the fundamental energy gap in $(PMA)_2CuBr_4$ is indirect with a value of 2.23 eV under ambient conditions.

Previous studies on this material[10,33] identified a fundamental band gap, with a value of approximately 1.80 eV under ambient conditions. According to our studies, this value actually corresponds to the d-d band in the perovskite.[54] The d–d band in perovskites refers to an electronic transition involving the d orbitals of transition metal ions in the structure. This transition can influence the optical absorption and emission properties of perovskites. However, in this case the d–d absorption occurs in the infrared range, making it invisible to the naked eye. Therefore, it is not discussed in detail in the context of thermo- and piezo-chromism of the studied materials.

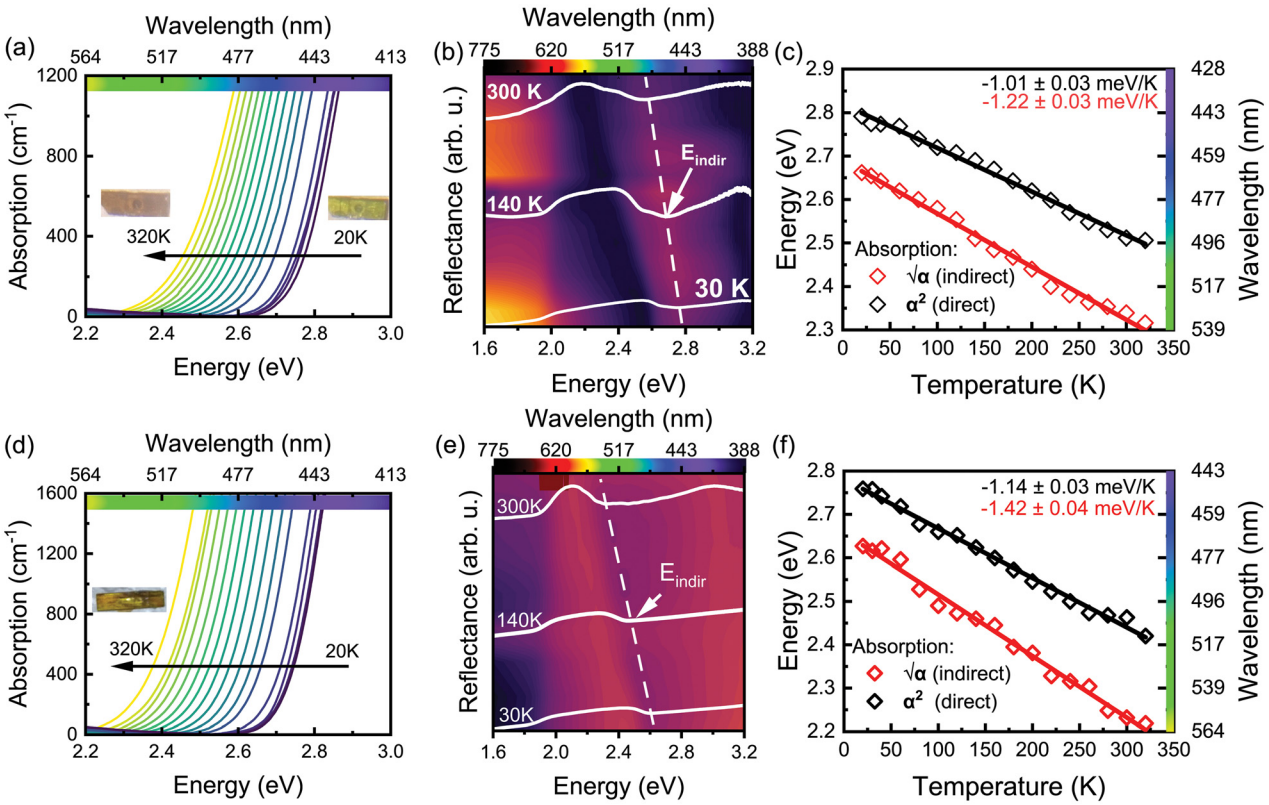

Fig. 1 Temperature dependence of (a) α, (b) R spectra for $(PMA)_2CuBr_4$ and (d) α, (e) R measurements for $(PMA)_2CuCl_4$. Indirect (open red diamonds) and direct (open black diamonds) gaps extracted from α measurements as a function of temperature for (c) $(PMA)_2CuBr_4$ and (f) $(PMA)_2CuCl_4$.

Fig. 1(d) shows the α spectra of $(PMA)_2CuCl_4$ measured from 20 to 320 K, and Fig. 1(e) illustrates the R spectra collected from 30 to 320 K. The α measurements reveal a linear narrowing of both the direct and indirect energy gaps with temperature, with a reduction of 303 meV ($\sim$51 nm from 444 to 495 nm) and 366 meV ($\sim$70 nm from 466 to 536 nm), respectively, from 20 to 320 K. This narrowing causes visible thermochromism, shifting from green at 20 K to yellow at 320 K. Similar to the previous considerations for $(PMA)_2CuBr_4$, the reduction in the energy gap and the color change are confirmed through R measurements. However, the presence of a transparency region near the indirect transition complicates the precise determination of the transition position at each temperature for the $(PMA)_2CuCl_4$ perovskite. Comparing the α^2 and $\sqrt{\alpha}$ spectra with the R spectra suggests that the fundamental energy gap in $(PMA)_2CuCl_4$ is indirect with a value of 2.33 eV under ambient conditions.

According to the previous studies,[55] an exciton emission for $(PMA)_2CuCl_4$ is observed at 2.12 eV under ambient conditions. This emission is consistent with the fundamental band gap of 2.33 eV determined in this work as there can be a few mechanisms, which can be responsible for the Stokes shift between emission and absorption, see ref. 56–60.

2.2. Piezochromism in $(PMA)_2CuBr_4$ and $(PMA)_2CuCl_4$ halide perovskites

To investigate piezochromism, transmission spectra under hydrostatic pressure were measured. Fig. 2(a) shows the normalized transmission spectra for $(PMA)_2CuBr_4$ as a function of hydrostatic pressure at room temperature. It can be observed that, as the pressure in the diamond anvil cell (DAC) increases, the band gap of $(PMA)_2CuBr_4$ shifts to lower energies (redshifts), similar to other perovskite materials.[61–63] However, this shift is significantly larger compared to other semiconductors.[64,65] The observed redshift is attributed to band gap narrowing in $(PMA)_2CuBr_4$ under hydrostatic pressure, resulting in a $\sim$400 meV shift ($\sim$90 nm from 482 to 572 nm) up to 10.94 GPa. The decompression process is shown in Fig. S7 in the SI, from which it can be concluded that, during pressure release in the DAC, the band gap of $(PMA)_2CuBr_4$ remains consistent with the data obtained during compression.

This pressure-induced shift in the band gap is accompanied by a visible piezochromic effect. As pressure increases, the color of the material changes, reflecting corresponding shifts in its optical properties. Specifically, the crystal color of $(PMA)_2CuBr_4$ transitions from yellow at 0.00 GPa to red/black at 10.94 GPa, consistent with the observed band gap narrowing. This visible piezochromism results directly from the pressure-induced modification of the material's electronic structure above the band gap, which alters the absorption spectrum, consequently changing the material's perceived color.

The change in the band gap, obtained from pressure-induced transmission spectra, is shown in Fig. 2(b). As seen, the pressure coefficients for $(PMA)_2CuBr_4$ were found to be $\alpha_I = -47 \pm 7$ and $\alpha_{II} = -30 \pm 2$ meV/GPa. The linear fitting used to extract the pressure coefficients from the data was performed

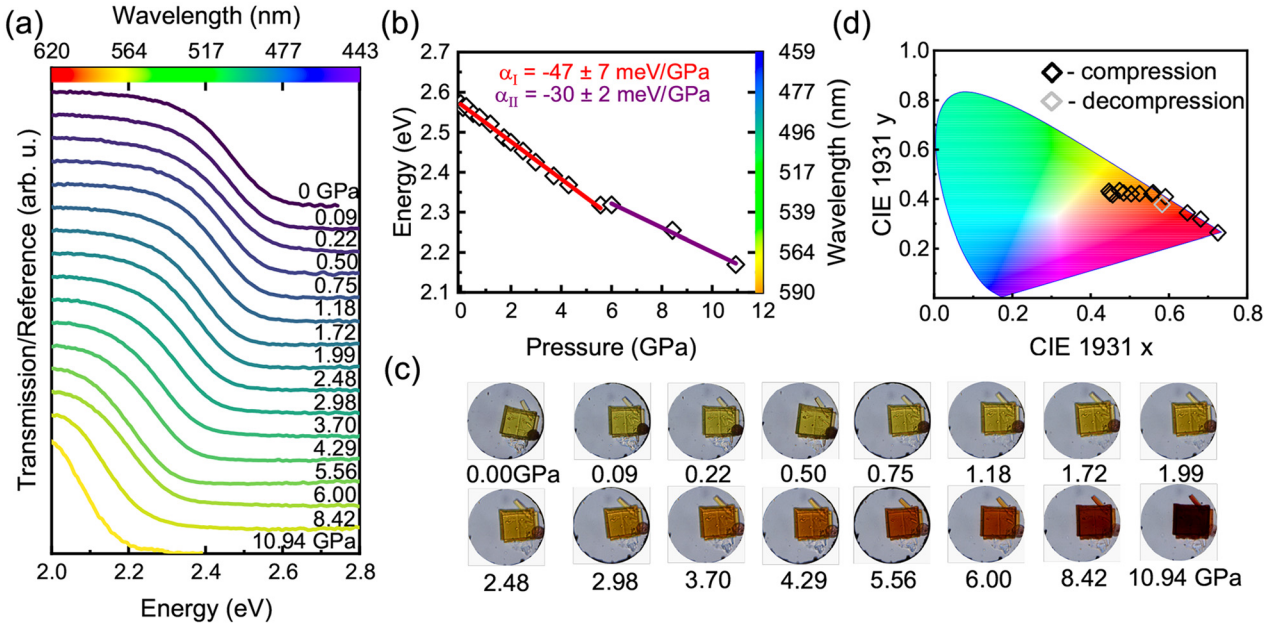

Fig. 2 (a) Transmission spectra showing the near absorption edge of $(PMA)_2CuBr_4$ under ambient conditions. (b) Band gap change as a function of pressure derived from the transmission spectra. (c) Optical micrographs of $(PMA)_2CuBr_4$ in DAC. (d) Pressure-dependent chromaticity coordinates shown in the CIE 1931 format.

in the range of 0.00 to 5.56 GPa for the first phase (P1), and in the range of 6.00 to 10.94 GPa for the second phase (P2). This transition change is attributed to a reduction in structural symmetry and a layer slip in the 2D structure caused by a tilting rotation of the octahedral perovskites.[66] According to previous studies for this material, $(PMA)_2CuBr_4$ exhibits no significant structural phase transitions up to 40 GPa which is associated with the protection of the organic cations by the amino group.[10]

Fig. 2(c) presents optical micrographs of the $(PMA)_2CuBr_4$ sample mounted in the DAC. The crystals' color change from yellow at 0.00 GPa to red/black at 10.94 GPa directly correlates with the band gap narrowing observed in the absorption edge. To further visualize the piezochromic effect, Fig. 2(d) illustrates the CIE 1931 chromaticity diagram.

Fig. 3(a) presents the normalized transmission spectra of $(PMA)_2CuCl_4$ under hydrostatic pressure at 300 K. Similar to the behavior observed for $(PMA)_2CuBr_4$, the band gap of $(PMA)_2CuCl_4$ redshifts with increasing pressure, decreasing by ~330 meV (~70 nm from 476 to 546 nm) up to 10.86 GPa. This indicates that the presence of PMA significantly enhances the structural stability of the material, as is the case of $(PMA)_2CuBr_4$, allowing higher pressures to be applied until irreversible amorphization occurs. During decompression, the band gap of $(PMA)_2CuCl_4$ remains consistent with the data obtained during compression. The pressure coefficients for $(PMA)_2CuCl_4$ were determined to be $\alpha_I = -53 \pm 3$ and $\alpha_{II} = -23 \pm 2$ meV/GPa for P1 and P2, respectively. The pressure coefficient for P1 is slightly larger than that for $(PMA)_2CuBr_4$, whereas for P2 it is smaller. A linear fit was applied to extract these coefficients, with the fitting range set to 0.00–4.43 GPa for P1 and 5.46–10.86 GPa for P2, respectively. As in $(PMA)_2CuBr_4$, the change in the pressure coefficient can be attributed to a phase transition, but a detailed analysis of this phase transition is beyond the scope of this article. Fig. 3(c) displays optical micrographs of $(PMA)_2CuCl_4$. The observed transition of the crystal color from yellow at 0.00 GPa to red/orange at 10.86 GPa is consistent with the band gap narrowing determined from the absorption edge region. Furthermore, to emphasize the thermo- and piezo-chromic effects, the CIE 1931 chart is shown in Fig. 3(d).

2.3. Discussion

In $(PMA)_2CuCl_4$ and $(PMA)_2CuBr_4$ perovskite materials, chlorine (Cl) and bromine (Br) have distinct effects on the materials' optical, electronic, and structural properties. Br has a larger ionic radius (1.96 Å) compared to Cl (1.81 Å), which leads to larger lattice parameters in bromine-based perovskites. This is a well-known chemical trend, which is observed for many crystals including 3D and 2D perovskites.[67] In terms of the optical and electronic properties, Cl-based perovskites typically exhibit a wider band gap absorbing light at shorter wavelengths, while Br-based perovskites have a narrower band gap,[68] this is also true for $(PMA)_2CuX_4$ (X = Br and Cl), although the gap narrowing upon replacement of Cl by Br is only 110 meV, while for other perovskites it is much larger.[69–71]

In these studies, it is worth emphasizing that the band gap tuning induced by the change of composition (*i.e.*, chemical tuning by substituting Cl with Br) is much smaller than the band gap tuning induced by physical factors (*i.e.*, temperature – thermochromism and pressure – piezochromism). The great advantage of the observed phenomenon of thermochromism

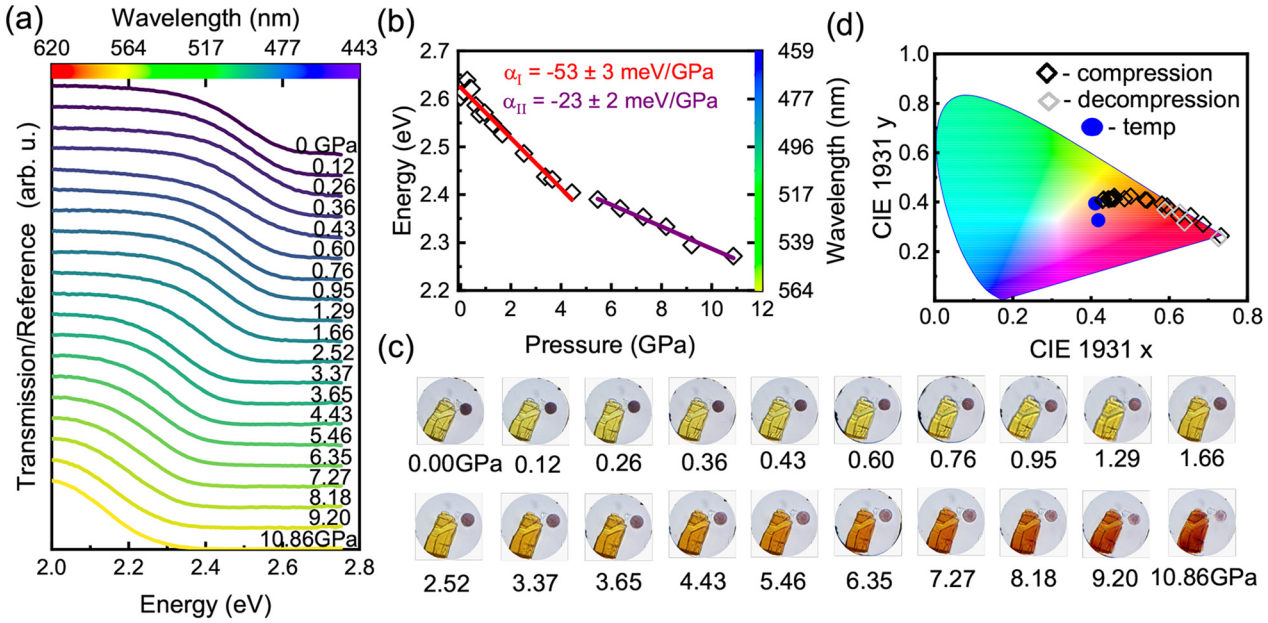

Fig. 3 (a) Transmission spectra showing the near absorption edge of $(PMA)_2CuCl_4$ under ambient conditions. (b) Band gap change as a function of pressure derived from transmission spectra. (c) Optical micrographs of $(PMA)_2CuCl_4$ in DAC. (d) Pressure-dependent chromaticity coordinates shown in the CIE 1931 format.

and piezochromism in these materials is the linear dependence of the absorption edge on external stimuli, which is not typical for many other perovskites. A continuous change in the energy gap with temperature does not indicate the presence of a phase transition. In general, phase transitions in perovskites often lead to a non-monotonic change in the energy gap.[72–74] Linear temperature dependence is crucial in thermo-devices, as it simplifies calibration and operation, ensuring predictable, consistent performance. Such sensors maintain stability in controlled environments and provide accurate data across a wide temperature range. Additionally, they are easy to integrate into systems that do not require high sensitivity to small temperature changes, making them a cost-effective solution for many applications.

Thermochromism and piezochromism both involve color changes in $(PMA)_2CuCl_4$ and $(PMA)_2CuBr_4$ materials, but they are driven by different stimuli – temperature and mechanical stress, respectively. These phenomena are closely related to interactions between electrons and phonons, as well as changes in the crystal lattice parameters. In thermochromism, the increase in lattice parameters caused by the increase in temperature leads to a narrowing of the energy gap, and additionally, the increase in the phonon population affects the narrowing of the energy gap through electron–phonon interactions. In piezochromism, we also deal with a narrowing of the energy gap, but the hydrostatic pressure leads to a decrease in the crystal volume (*i.e.* a decrease in lattice parameters, which is opposite to the thermal expansion of the lattice parameters with increasing temperature). The thermal energy of the crystal does not change during measurements under hydrostatic pressure because the measurements are performed at the same temperature, but the phonon dispersion changes under hydrostatic pressure and therefore the electron–phonon interaction may also change, which may also affect the energy gap narrowing.

The simple comparison of thermo- and piezo-chromism in $(PMA)_2CuCl_4$ and $(PMA)_2CuBr_4$ crystals indicates that the changes in lattice parameters induced by temperature and pressure are not equivalent, even if electron–phonon interactions play an important role in both thermo- and piezo-chromism. This means that the narrowing of the energy gap in the studied perovskites is a complex issue, and the electron–phonon interaction can certainly play a significant role in it and requires deeper research, including theoretical studies.

3 Conclusion

In conclusion, a comprehensive study of the thermo- and piezochromism of $(PMA)_2CuCl_4$ and $(PMA)_2CuBr_4$ has been carried out. We observed significant reductions in the energy gap: 366 meV (~70 nm from 466 to 536 nm) for $(PMA)_2CuCl_4$ and 426 meV (~87 nm from 472 to 559 nm) for $(PMA)_2CuBr_4$ across the 20–320 K temperature range. Additionally, pressure-dependent energy gap reductions were observed: 330 meV (~70 nm from 476 to 546 nm) up to 10.94 GPa for $(PMA)_2CuCl_4$ and by 400 meV (~90 nm from 482 to 572 nm) up to 10.86 GPa for $(PMA)_2CuBr_4$) which manifests as a visible color change. The observed changes in the band gap are continuous without any sudden jumps, which is a great advantage in terms of using these materials in thermochromic and piezochromic sensors. The fundamental energy gap for both was found to be indirect,

with values of 2.33 eV for $(PMA)_2CuCl_4$ and 2.23 eV for $(PMA)_2CuBr_4$ under ambient conditions. Compared to other halide perovskites, both materials possess one of the highest band gap tunabilities reported to date. The hydrophobic PMA cation stabilizes the material by preventing moisture absorption and structural degradation due to environmental factors and ensuring that the lattice remains stable under stress. This structural stability allows for controlled band gap tunability with temperature or pressure variations, making these perovskites promising candidates for color or pressure sensing applications.

Author contributions

Rafał Bartoszewicz carried out the experimental work, data analyses, visualization and writing the original draft. He was also equally involved in conceiving the concept and methodology. Muhammad Danang Birowosuto, Jan-Albert Zienkiewicz, Sri Hartati, Arramel were responsible for providing $(PMA)_2CuCl_4$ and $(PMA)_2CuBr_4$ samples and structural measurements. Jan Kopaczek was responsible for the methodology. Robert Kudrawiec conceived the concept and supervised the work. All authors discussed the research progress and contributed to editing the paper.

Conflicts of interest

There are no conflicts to declare.

Data availability

The data supporting this study have been included as part of the SI.

Detailed materials and methods; experimental layout; additional XRD patterns, FTIR, Raman, XPS spectra for $(PMA)_2CuCl_4$ and $(PMA)_2CuBr_4$ obtained at ambient conditions; optimized geometric structure of $(PMA)_2CuCl_4$ built based on CIF; analysis of α^2 and $\sqrt{\alpha}$ from absorption spectra at 20 and 320 K, direct comparison of reflectance spectra with α^2 and $\sqrt{\alpha}$ at 30 K, position of d–d band and band gap, spectral position of band gap during decompression for $(PMA)_2CuCl_4$ and $(PMA)_2CuBr_4$; determination of the absorption edge. See DOI: **https://doi.org/10.1039/d5tc02326b**

Acknowledgements

This work was supported by the National Science Centre Poland, OPUS Grant no. 2020/39/B/ST3/02704.

References

1 H. Dong, C. Zhang, X. Liu, J. Yao and Y. S. Zhao, *Chem. Soc. Rev.*, 2020, **49**, 951–982.
2 A. Fakharuddin, M. K. Gangishetty, M. Abdi-Jalebi, S.-H. Chin, A. R. bin Mohd Yusoff, D. N. Congreve, W. Tress, F. Deschler, M. Vasilopoulou and H. J. Bolink, *Nat. Electron.*, 2022, **5**, 203–216.
3 C. Sun, Y. Jiang, M. Cui, L. Qiao, J. Wei, Y. Huang, L. Zhang, T. He, S. Li, H.-Y. Hsu, C. Qin, R. Long and M. Yuan, *Nat. Commun.*, 2021, **12**, 2207.
4 L. Zhang, C. Sun, T. He, Y. Jiang, J. Wei, Y. Huang and M. Yuan, *Light: Sci. Appl.*, 2021, **10**, 61.
5 C. Qin, A. S. D. Sandanayaka, C. Zhao, T. Matsushima, D. Zhang, T. Fujihara and C. Adachi, *Nature*, 2020, **585**, 53–57.
6 E. Yassitepe, Z. Yang, O. Voznyy, Y. Kim, G. Walters, J. A. Castañeda, P. Kanjanaboos, M. Yuan, X. Gong, F. Fan, J. Pan, S. Hoogland, R. Comin, O. M. Bakr, L. A. Padilha, A. F. Nogueira and E. H. Sargent, *Adv. Funct. Mater.*, 2016, **26**, 8757–8763.
7 W. Chen, Z. Huang, H. Yao, Y. Liu, Y. Zhang, Z. Li, H. Zhou, P. Xiao, T. Chen, H. Sun, J. Huang and Z. Xiao, *Nat. Photonics*, 2023, **17**, 401–407.
8 N. Marchal, W. Van Gompel, M. C. Gélvez-Rueda, K. Vandewal, K. Van Hecke, H.-G. Boyen, B. Conings, R. Herckens, S. Maheshwari, L. Lutsen, C. Quarti, F. C. Grozema, D. Vanderzande and D. Beljonne, *Chem. Mater.*, 2019, **31**, 6880–6888.
9 G. E. Eperon, S. D. Stranks, C. Menelaou, M. B. Johnston, L. M. Herz and H. J. Snaith, *Energy Environ. Sci.*, 2014, **7**, 982–988.
10 X. Zhan, X. Jiang, P. Lv, J. Xu, F. Li, Z. Chen and X. Liu, *Angew. Chem., Int. Ed.*, 2022, **61**, e202205491.
11 W. S. Yang, J. H. Noh, N. J. Jeon, Y. C. Kim, S. Ryu, J. Seo and S. I. Seok, *Science*, 2015, **348**, 1234–1237.
12 J. Yang, Q. Bao, L. Shen and L. Ding, *Nano Energy*, 2020, **76**, 105019.
13 I. Kopacic, B. Friesenbichler, S. F. Höfler, B. Kunert, H. Plank, T. Rath and G. Trimmel, *ACS Appl. Energy Mater.*, 2018, **1**, 343–347.
14 H. C. Sansom, G. Longo, A. D. Wright, L. R. V. Buizza, S. Mahesh, B. Wenger, M. Zanella, M. Abdi-Jalebi, M. J. Pitcher, M. S. Dyer, T. D. Manning, R. H. Friend, L. M. Herz, H. J. Snaith, J. B. Claridge and M. J. Rosseinsky, *J. Am. Chem. Soc.*, 2021, **143**, 3983–3992.
15 Y. Liao, H. Liu, W. Zhou, D. Yang, Y. Shang, Z. Shi, B. Li, X. Jiang, L. Zhang, L. N. Quan, R. Quintero-Bermudez, B. R. Sutherland, Q. Mi, E. H. Sargent and Z. Ning, *J. Am. Chem. Soc.*, 2017, **139**, 6693–6699.
16 D. Cortecchia, H. A. Dewi, J. Yin, A. Bruno, S. Chen, T. Baikie, P. P. Boix, M. Grätzel, S. Mhaisalkar, C. Soci and N. Mathews, *Inorg. Chem.*, 2016, **55**, 1044–1052.
17 Z. Shi, J. Guo, Y. Chen, Q. Li, Y. Pan, H. Zhang, Y. Xia and W. Huang, *Adv. Mater.*, 2017, **29**, 1605005.
18 X. Li, X. Zhong, Y. Hu, B. Li, Y. Sheng, Y. Zhang, C. Weng, M. Feng, H. Han and J. Wang, *J. Phys. Chem. Lett.*, 2017, **8**, 1804–1809.
19 X.-P. Cui, K.-J. Jiang, J.-H. Huang, Q.-Q. Zhang, M.-J. Su, L.-M. Yang, Y.-L. Song and X.-Q. Zhou, *Synth. Met.*, 2015, **209**, 247–250.
20 A. Elattar, H. Suzuki, R. Mishima, K. Nakao, H. Ota, T. Nishikawa, H. Inoue, A. K. K. Kyaw and Y. Hayashi, *J. Mater. Chem. C*, 2021, **9**, 3264–3270.

21 H. Tsai, W. Nie, J.-C. Blancon, C. C. Stoumpos, R. Asadpour, B. Harutyunyan, A. J. Neukirch, R. Verduzco, J. J. Crochet, S. Tretiak, L. Pedesseau, J. Even, M. A. Alam, G. Gupta, J. Lou, P. M. Ajayan, M. J. Bedzyk and M. G. Kanatzidis, *Nature*, 2016, **536**, 312–316.
22 I. C. Smith, E. T. Hoke, D. Solis-Ibarra, M. D. McGehee and H. I. Karunadasa, *Angew. Chem., Int. Ed.*, 2014, **53**, 11232–11235.
23 Q.-Q. Sun, Q. Li, H.-Y. Li, M.-M. Zhang, M.-E. Sun, S. Li, Z. Quan and S.-Q. Zang, *Chem. Commun.*, 2021, **57**, 2372–2375.
24 F.-F. Gao, H. Song, Z.-G. Li, Y. Qin, X. Li, Z.-Q. Yao, J.-H. Fan, X. Wu, W. Li and X.-H. Bu, *Angew. Chem., Int. Ed.*, 2023, **62**, e202218675.
25 X. Wu, Y. Sun, L. Wang, Y. Huang, J. Wang, Y. Yuan, U. Shahzadi, R. Fu, K. Wang and H. Guo, *Adv. Opt. Mater.*, 2025, **13**, 2402136.
26 M. De Bastiani, M. I. Saidaminov, I. Dursun, L. Sinatra, W. Peng, U. Buttner, O. F. Mohammed and O. M. Bakr, *Chem. Mater.*, 2017, **29**, 3367–3370.
27 S. Liu, Y. Li, Y. Wang, K. M. Yu, B. Huang and C. Y. Tso, *Adv. Sci.*, 2022, **9**, 2106090.
28 O. Mapazi, P. K. Matabola, R. M. Moutloali and C. J. Ngila, *Sens. Actuators, B*, 2017, **252**, 671–679.
29 M. Cinquino, C. T. Prontera, A. Giuri, M. Pugliese, R. Giannuzzi, A. Maggiore, D. Altamura, F. Mariano, G. Gigli, C. Esposito Corcione, C. Giannini, A. Rizzo, L. De Marco and V. Maiorano, *Adv. Mater.*, 2024, **36**, 2307564.
30 C. Pareja-Rivera and D. Solis-Ibarra, *Adv. Opt. Mater.*, 2021, **9**, 2100633.
31 A. Singh and S. Satapathi, *Adv. Opt. Mater.*, 2021, **9**, 2101062.
32 W. Ning, X.-G. Zhao, J. Klarbring, S. Bai, F. Ji, F. Wang, S. I. Simak, Y. Tao, X.-M. Ren, L. Zhang, W. Huang, I. A. Abrikosov and F. Gao, *Adv. Funct. Mater.*, 2019, **29**, 1807375.
33 X. Li, B. Li, J. Chang, B. Ding, S. Zheng, Y. Wu, J. Yang, G. Yang, X. Zhong and J. Wang, *ACS Appl. Energy Mater.*, 2018, **1**, 2709–2716.
34 K. Zulfa, B. Zahara, A. Akmal Afkauni, P. Yuniar Diah Maulida, S. Hartati, I. Mulyani, A. Yudhowijoyo, L. Jaya Diguna, M. Haris Mahyuddin, D. Onggo, M. Danang Birowosuto and A. Arramel, *Mater. Today: Proc.*, 2024, DOI: 10.1016/j.matpr.2024.03.058.
35 G. Liu, L. Kong, W. Yang and H.-K. Mao, *Mater. Today: Proc.*, 2019, **27**, 91–106.
36 W. Zhao, G. Xiao and B. Zou, *Aggregate*, 2024, **5**, e461.
37 S. Wang, J. Ma, W. Li, J. Wang, H. Wang, H. Shen, J. Li, J. Wang, H. Luo and D. Li, *J. Phys. Chem. Lett.*, 2019, **10**, 2546–2553.
38 Y. Zhu, J. Buitenhuis, B. Förster, M. R. Vetrano and E. Koos, *ACS Appl. Nano Mater.*, 2023, **6**, 4661–4671.
39 A. Celeste and F. Capitani, *J. Appl. Phys.*, 2022, **132**, 220903.
40 X.-Z. Zhao, F.-F. Gao, W. Li, Z.-G. Li, Y. Zhang, K. Li, H. Hu, W. Cai, J. Zhang and X.-H. Bu, *J. Mater. Chem. C*, 2024, **12**, 4599–4605.
41 J. Xu, S. Yu, X. Shang and X. Chen, *Adv. Photonics Res.*, 2023, **4**, 2200193.
42 J. Ning, L. Zheng, W. Lei, S. Wang, J. Xi and J. Yang, *Phys. Chem. Chem. Phys.*, 2022, **24**, 16003–16010.
43 Y. Zhou, D. Zhao, F. Wang, Y. Shi, Z. Ma, R. Fu, K. Wang, Y. Sui, Q. Dong, G. Xiao and B. Zou, *Phys. Rev. Mater.*, 2023, **7**, 074002.
44 P. Steeger, M. Adnan, T. Deilmann, X. Li, S. Müller, K. Skrzynska, M. Hanfland, E. Kolesnikov, J. Kösters, T. Block, R. Schmidt, I. Kupenko, C. Sanchez-Valle, G. Vijaya Prakash, S. Michaelis de Vasconcellos and R. Bratschitsch, *J. Am. Chem. Soc.*, 2024, **146**, 23205–23211.
45 L. Zhang, L. Wu, K. Wang and B. Zou, *Adv. Sci.*, 2019, **6**, 1801628.
46 N. Hassan, S. Nagaraja, S. Saha, K. Tarafder and N. Ballav, *Chem. Sci.*, 2024, **15**, 4075–4085.
47 R. F. I. Josey and J. L. Fenton, *Inorg. Chem.*, 2024, **63**, 6026–6032.
48 Y.-H. Liu, Y.-F. Wu, L.-J. Feng, R.-R. Zhao, S.-X. Wang, M.-M. Zhang, D.-Y. Wang, X.-W. Kong and X.-W. Lei, *Chem. Commun.*, 2023, **59**, 10267–10270.
49 I. Vurgaftman, J. R. Meyer and L. R. Ram-Mohan, *J. Appl. Phys.*, 2001, **89**, 5815–5875.
50 G. Mannino, I. Deretzis, E. Smecca, A. La Magna, A. Alberti, D. Ceratti and D. Cahen, *J. Phys. Chem. Lett.*, 2020, **11**, 2490–2496.
51 F. Ji, J. Klarbring, F. Wang, W. Ning, L. Wang, C. Yin, J. S. M. Figueroa, C. K. Christensen, M. Etter, T. Ederth, L. Sun, S. I. Simak, I. A. Abrikosov and F. Gao, *Angew. Chem.*, 2020, **132**, 15303–15306.
52 J. Bhosale, A. K. Ramdas, A. Burger, A. Muñoz, A. H. Romero, M. Cardona, R. Lauck and R. K. Kremer, *Phys. Rev. B*, 2012, **86**, 195208.
53 Y. P. Varshni, *Physica*, 1967, **34**, 149–154.
54 A. Jaffe, Y. Lin, W. L. Mao and H. I. Karunadasa, *J. Am. Chem. Soc.*, 2015, **137**, 1673–1678.
55 A. Arramel, A. D. Fauzi, X. Yin, C. S. Tang, M. H. Mahyuddin, M. F. Sahdan, M. Aminah, D. Onggo, G. Shukri, C. Diao, H. Wang, M. D. Birowosuto, A. T. S. Wee and A. Rusydi, *Commun. Mater.*, 2021, **2**, 1–12.
56 J. A. Peters, Z. Liu, M. C. De Siena, M. G. Kanatzidis and B. W. Wessels, *J. Lumin.*, 2022, **243**, 118661.
57 T. Yamada, T. Aharen and Y. Kanemitsu, *Phys. Rev. Lett.*, 2018, **120**, 057404.
58 F. Dybala, R. Kudrawiec, M. P. Polak, A. P. Herman, A. Sieradzki and M. Maczka, *Mater. Adv.*, 2025, **6**, 569–578.
59 A. Pieniazek, F. Dybala, M. P. Polak, U. Przypis, A. P. Herman, J. Kopaczek and R. Kudrawiec, *J. Phys. Chem. Lett.*, 2023, **14**, 6470–6476.
60 H. He, Q. Yu, H. Li, J. Li, J. Si, Y. Jin, N. Wang, J. Wang, J. He, X. Wang, Y. Zhang and Z. Ye, *Nat. Commun.*, 2016, **7**, 10896.
61 H. Li, D. Wines, B. Chen, K. Yumigeta, Y. M. Sayyad, J. Kopaszek, S. Yang, C. Ataca, E. H. Sargent and S. Tongay, *ACS Appl. Mater. Interfaces*, 2021, **13**, 44964–44971.
62 C. Wolf and T.-W. Lee, *Mater. Today Energy*, 2018, **7**, 199–207.
63 M. Maczka, S. Sobczak, P. Ratajczyk, F. F. Leite, W. Paraguassu, F. Dybala, A. P. Herman, R. Kudrawiec and A. Katrusiak, *Chem. Mater.*, 2022, **34**, 7867–7877.

64 N. E. Christensen and I. Gorczyca, *Phys. Rev. B:Condens. Matter Mater. Phys.*, 1994, **50**, 4397–4415.
65 P. E. Van Camp, V. E. Van Doren and J. T. Devreese, *Phys. Rev. B:Condens. Matter Mater. Phys.*, 1990, **41**, 1598–1602.
66 S. Guo, K. Bu, J. Li, Q. Hu, H. Luo, Y. He, Y. Wu, D. Zhang, Y. Zhao, W. Yang, M. G. Kanatzidis and X. Lü, *J. Am. Chem. Soc.*, 2021, **143**, 2545–2551.
67 W. Ning and F. Gao, *Adv. Mater.*, 2019, **31**, 1900326.
68 Y. Liu, Z. Yang, D. Cui, X. Ren, J. Sun, X. Liu, J. Zhang, Q. Wei, H. Fan, F. Yu, X. Zhang, C. Zhao and S. F. Liu, *Adv. Mater.*, 2015, **27**, 5176–5183.
69 M. Szafranski, *J. Mater. Chem. A*, 2024, **12**, 2391–2399.
70 K. Fedoruk, D. Drozdowski, M. Maczka, J. K. Zareba, D. Stefanska, A. Gagor and A. Sieradzki, *Inorg. Chem.*, 2022, **61**, 15520–15531.
71 R. Comin, G. Walters, E. S. Thibau, O. Voznyy, Z.-H. Lu and E. H. Sargent, *J. Mater. Chem. C*, 2015, **3**, 8839–8843.
72 F. Ruf, M. F. Aygüler, N. Giesbrecht, B. Rendenbach, A. Magin, P. Docampo, H. Kalt and M. Hetterich, *APL Mater.*, 2019, **7**, 031113.
73 M. Armer, P. Dörflinger, A. Weis, C. Büchner, A. Gottscholl, J. Höcker, K. Frank, L. Nusser, M. T. Sirtl, B. Nickel, T. Bein and V. Dyakonov, *Adv. Photonics Res.*, 2023, **4**, 2300017.
74 S. Neutzner, A. R. Srimath Kandada, G. Lanzani and A. Petrozza, *J. Mater. Chem. C*, 2016, **4**, 4630–4633.

